Published in final edited form as:
J Biomed Mater Res A. 2013 June ; 101(6): 1571–1581. doi:10.1002/jbm.a.34462.

Mineralization Induction Effects of Osteopontin, Bone Sialoprotein, and Dentin Phosphoprotein on a Biomimetic Collagen Substrate

Kevin M. Zurick[a], **Chunlin Qin**[c], and **Matthew T. Bernards**[a,b,*]

[a]Department of Chemical Engineering, University of Missouri, Columbia, MO 65211

[b]Department of Biological Engineering, University of Missouri, Columbia, MO 65211

[c]Department of Biomedical Sciences, Baylor College of Dentistry, Texas A&M Health Science Center, Dallas, TX 75246

Abstract

Native bone tissue is composed of a matrix of collagen, non-collagenous proteins, and calcium phosphate minerals, which are primarily hydroxyapatite (HA). The SIBLING (small integrin-binding ligand, N-linked glycoprotein) family of proteins is the primary non-collagenous protein group found in mineralized tissues. In this work, the mineralization induction capabilities of three of the SIBLING members, bone sialoprotein (BSP), osteopontin (OPN), and the calcium binding subdomain of dentin sialophosphoprotein, dentin phosphoprotein (DPP), are directly compared on a biomimetic collagen substrate. A self-assembled, loosely aligned collagen fibril substrate was prepared and then ^{125}I radiolabeled adsorption isotherms were developed for BSP, OPN, and DPP. The results showed that BSP exhibited the highest binding capacity for collagen at lower concentrations, followed by DPP and OPN. However, at the highest concentrations all three proteins had similar adsorption levels. The adsorption isotherms were then used to identify conditions that resulted in identical amounts of adsorbed protein. These substrates were prepared and placed in simulated body fluid for 5 hours, 10 hours, and 24 hours at 37°C. The resulting mineral morphology was assessed by atomic force microscopy and the composition was determined using photochemical assays. Mineralization was seen in the presence of all of the proteins. However, DPP was seen to be the only protein that formed individual mineral nodules similar to those seen in developing bone. This suggests that DPP plays a significant role in the biomineralization process and that the incorporation of DPP into tissue engineering constructs may facilitate the induction of biomimetic mineral formation.

Keywords

SIBLING proteins; biomineralization; calcium phosphates

Introduction

In native bone tissue 10-30% of the tissue mass is proteinaceous and the remaining 70-90% is comprised of calcium phosphate mineral, which is primarily hydroxyapatite (HA).[1] The protein component of bone has been shown to be ~90% collagenous, while the remaining 10% of the protein content is believed to play a role in bone formation, growth, repair, and cellular adhesion to the matrix.[1,2] The primary group of non-collagenous proteins found in

*Corresponding Authors: Matthew T. Bernards: bernardsm@missouri.edu.

bone are the SIBLING (small integrin-binding ligand, *N*-linked glycoprotein) family of proteins and they are believed to play a key role in these processes.[2]

The SIBLING family of proteins consists of five members: osteopontin (OPN), matrix extracellular phosphoglycoprotein (MEPE), bone sialoprotein (BSP), dentin matrix protein 1 (DMP1), and dentin sialophosphoprotein (DSPP). The SIBLING proteins have a number of shared characteristics including a collagen binding domain, a HA binding domain, and a cell binding arganine-glycine-aspartic acid (RGD) sequence. Additionally, they are all located on the same human chromosome (4q21).[2] All of the proteins are acidic and contain a high degree of random coil structure. Additionally, all of the proteins are post-translationally phosphorylated and have been immunolocalized in mineralized tissues.[2-5] Together, these characteristics suggest that the SIBLING family of proteins play an important role in bone development by facilitating cellular adhesion, mineral nucleation, and mineral maturation.

Researchers are still trying to elucidate the exact roles that each protein plays in natural bone development, but a recent review summarized the current consensus for each protein.[2] MEPE has been shown to be a potent inhibitor of mineralization both *in vitro* and *in vivo* and therefore is not expected to play a role in the induction of biomineralization. DMP1 is believed to regulate the mineralization process, possibly mediating the transformation of amorphous calcium phosphate to crystalline HA. OPN has been shown to either inhibit or induce mineralization based on its phosphorylation state, but most likely regulates the mineralization process in bone. DSPP is a highly negatively charged molecule that strongly binds calcium ions and may induce the biomineralization process. Furthermore, dentin phosphoprotein (DPP) is the cleavage fragment of DSPP that contains the unique series of repeat aspartic acid-serine-serine (RSS) amino acids that are responsible for this calcium binding. Finally, BSP has been identified as the most likely SIBLING protein responsible for apatite nucleation, although this is not definitive.

In this investigation OPN, BSP, and DPP are studied to better formalize the individual roles that these proteins play in biomineralization. MEPE is not being considered at this time due to its known inhibitory role and DMP1 is not being investigated due to its perceived role in mineral maturation. While OPN is also perceived to play a regulatory role, it has been immunolocalized in the collagen matrix ahead of developing bone and uncertainty remains regarding its mineralization induction properties. DPP has been shown to have the capacity to strongly bind calcium ions, indicating its potential for playing a role in biomineralization.[5,6] Furthermore, OPN and BSP have also been seen to be enriched at bone-implant interfacial sites.[1,2,7-11] This suggests that these three proteins are the most likely candidates responsible for inducing biomineralization of the collagen matrix in developing bone.

OPN was originally isolated from bone tissue and is comprised of 260-317 amino acids with a molecular weight of 45-75 kDa.[4] It exhibits Ca^{2+} chelating properties which are due to a high amount of phosphorylation and negative charge.[4,12] Depending on the degree of phosphorylation and concentration present, OPN has been shown to inhibit or encourage HA nucleation in an *in vitro* gelatin-gel system.[13] Since its initial discovery, OPN has since been found in other tissues beyond bone where calcium phosphate mineralization occurs.[2,4,12]

BSP was initially isolated from bone and is comprised of 281-327 amino acids with a molecular weight of 60-80 kDa.[3] Similar to OPN, BSP has strong Ca^{2+} chelating properties due to an overall negative charge and a high degree of phosphorylation.[3] Additionally, it has been shown that the collagen-BSP interaction promotes HA formation in several *in vitro* systems.[14,15] Specifically, BSP exhibits a binding preference for triple-helical collagen, and when bound to collagen it promotes HA nucleation *in vitro*.[14] Additionally, Gordon *et al.*

showed that BSP enhances both osteoblast differentiation and matrix mineralization *in vitro* in osteoblasts genetically engineered to overexpress BSP.[15]

DSPP was originally thought to only occur in dentin, but has since been found in bone tissue.[2,16] DSPP is cleaved into two fragments in bone and dentin, dentin phosphoprotein (DPP) and dentin sialoprotein (DSP).[17] DPP is a highly negatively charged molecule comprised of 751 amino acids in humans with a molecular weight of 100-140 kDa.[2,5] It also has a high degree of phosphorylation.[5,6,17] It is the major non-collagenous protein of the dentin extracellular matrix (ECM) and becomes soluble only after the ECM has been demineralized.[17] Additionally, it contains a highly repeated DSS (aspartic acid-serine-serine) group which is believed to aid in Ca^{2+} binding and subsequent HA mineralization. In one representative mineralization study, Milan *et al.* showed that DPP significantly promotes the rate of HA crystal growth when specifically bound to collagen I.[18]

The foci of this work are to determine the adsorption characteristics of OPN, BSP, and DPP to an aligned 2D collagen type I fibril matrix that resembles developing bone and to directly compare the mineralization induction effects of OPN, BSP, and DPP when specifically bound to this matrix. Multiple investigations have characterized the adsorption or binding of these proteins to various collagen coatings.[1,3-5,17] For example, our previous work probed OPN and BSP binding to a collagen type I tropocollagen coating on tissue culture polystyrene (TCPS).[19] However, there is noticeable variation in the levels of bound or adsorbed protein depending on the structure, type, and source of the collagen substrate. During bone formation, it has been shown that cells initially lay down a matrix composed of loosely aligned collagen type I fibrils, which are then mineralized.[1] A similar collagen assembly would therefore be the most biologically relevant for probing SIBLING induced biomineralization. Recently, Jiang and colleagues demonstrated the self-assembly of tropocollagen into loosely-aligned collagen fibrils with characteristic *D*-periodicity, similar to that found *in vivo*, using a mica substrate.[20] The interactions between the mica surface chemistry and tropocollagen molecules were found to guide the self-assembly process, leading to a good biomimetic collagen fibril platform for conducting biomineralization investigations.

The specific roles that OPN, DPP, and BSP play in mineral formation and growth have not been fully determined. This information is of interest in bone biology and it can be used to guide the development of bone tissue engineered materials. This is one of the first direct side-by-side studies of the mineralization capacities of SIBLING proteins on a substrate that mimics developing bone. The results suggest that while minerals were seen in the presence of all three SIBLING proteins, DPP was the only protein that formed distinct mineral nodules that most closely resemble those of developing bone. This suggests that DPP may be responsible for inducing biomineralization.

Materials and Methods

Materials

Ultrapure water (18.2 MΩ-cm) was obtained from a Millipore Synergy UV water purifier (Billerica, MA) and it was used for all experiments. Mica discs (10 mm diameter) were purchased from Ted Pella Inc. (Redding, CA) and were freshly cleaved immediately prior to use. Phosphate buffered saline (PBS, 150 mM, pH 7.4), KCl, NaCl, $NaHCO_3$, Na_2CO_3, KCl, K_2HPO_4, $MgCl_2$ Na_2SO_4, and tris(hydroxymethyl)aminomethane (Tris-HCl) were purchased from Thermo Fisher Scientific (Waltham, MA). KCl-Tris buffer was prepared by dissolving 50 mM Tris-HCl and 200 mM KCl in 18.2 MΩ-cm water and adjusting the pH to 7.4 with NaOH. Bovine serum albumin (BSA) with a purity of >96% was purchased from Sigma-Aldrich (Saint Louis, MO). Heat denatured BSA was prepared by heating a 1 mg/mL

solution of BSA in Tris-KCl buffer at 60 °C for 30 minutes. Type I collagen from rat tail with a purity of >90% was purchased from BD Biosciences (Bedford, MA). 4-(2-hydroxyethyl)-1-piperazineethanesulfonic acid (HEPES) was purchased from Sigma Aldrich. $CaCl_2$ and NaOH were purchased from Acros Organics (Pittsburgh, PA). The PiPer phosphate assay kit was purchased from Molecular Probes (Eugene, OR) and the QuantiChrom calcium assay kit was purchased from BioAssay Systems (Hayward, CA). 50% HNO_3 was obtained from Ricca Chemical Company (Arlington, TX) and diluted to 1.0 M using ultrapure water before use. Iodogen reagent was purchased from Pierce (Rockford, IL) and ^{125}I-Na was obtained from Amersham (Arlington Heights, IL).

SIBILING protein isolation procedures

BSP and OPN, were extracted from the tibiae of 10-week-old rats as described in detail previously.[21,22] The total bone protein extracts were subjected to multiple gel chromatography isolation/purification steps. The purity and identity of OPN and BSP were confirmed with polyacrylamide gel electrophoresis and Western immunoblots using antibodies specific to OPN and BSP.

DPP was extracted from the incisor dentin of 10-wk-old rats by standard procedures as described in detail elsewhere.[23,24] Briefly, the total rat dentin protein extract was subjected to gel chromatography, ion-exchange, and size-exclusion chromatography isolation/purification steps. Fractions containing DPP were combined, dialyzed, and lyophilized for use in this study. The purity of the collected DPP was confirmed by SDS-PAGE with Stains-All staining.

Collagen substrate preparation

Collagen-coated mica discs were prepared by adapting a previously established procedure.[20] Substrates were prepared by incubating freshly cleaved mica disks with 40 μL of a 0.3 mg/mL collagen solution in KCl-Tris buffer. The discs were covered with a Parafilm square immediately after applying the collagen solution and left overnight at room temperature. Following the overnight adsorption, the substrates were rinsed with ultrapure water and dried with filtered air. The presence of aligned collagen fibrils was confirmed using atomic force microscopy (AFM). AFM was performed on an Agilent 5400 (Agilent Technologies, Palo Alto, CA). Silicon cantilevers having a force constant of 0.2 N/m and a resonant frequency of 13 kHz were purchased from Budget Sensors (Bulgaria). Images were obtained in contact mode with a resolution of 1024×1024 pixels at a rate of 3.0 lines/second using a 10 μm scanner. Images were simultaneously recorded in topography and deflection modes. All images were acquired in air at room temperature. Gwyddion freeware was used to view and analyze the images.[25]

Radiolabeling procedure

BSP, OPN, and DPP were individually labeled with ^{125}I using iodogen reagent and a previously established procedure.[26] Briefly, 100 μg of iodogen was suspended in 35 μL of the desired protein solution to which 750 μCi of ^{125}I-Na (100 mCi/mL) was added. After 5 min, the mixture was transferred to a 20 cm Sephadex G25-150 column that had been equilibrated with PBS (pH 7.4). The column was then eluted with 15 mL of PBS and 500 μL fractions were collected. The radioactivity associated with each fraction was determined, and the highest count radiolabeled fraction for each protein was selected and used in all subsequent protein binding experiments.

Protein adsorption isotherms

Collagen-coated mica discs were prepared as previously described, then rinsed with 18.2 MΩ-cm water and soaked in 1 mg/mL heat-denatured BSA for 5 hours to block nonspecific protein binding.[125]I radiolabeled OPN, BSP, or DPP were added to 1.0 mg/mL solutions of unlabeled OPN, BSP, or DPP to obtain solutions with specific activities of 144.0, 124.2, and 116.0 counts per minute (cpm) per nanogram of protein, respectively. The collagen substrates were removed from the BSA solution and rinsed with 18.2 MΩ-cm water before being incubated with varying concentrations of BSP, DPP, or OPN solutions overnight at 4 °C in a humidified atmosphere. Afterwards, they were rinsed 3 times with KCl-Tris buffer to remove loosely bound proteins. The cpm radioactivity of all of the samples was measured with a Wizard 1470 automatic gamma counter (PerkinElmer, Waltham, MA). The amount of protein specifically adsorbed to the surface of the substrates was calculated by relating the cpm of each sample to the sample surface area and specific activity of each protein exposure solution. Each protein concentration adsorption experiment was repeated three times (n=3).

Mineralization using simulated body fluid

Mineralization on the collagen-coated mica discs with adsorbed proteins was probed using the modified simulated body fluid (m-SBF) described by Oyane *et al.*[27] Briefly, the reagents listed in Table 1 were dissolved in the order listed into 18.2 MΩ-cm water at 37 °C to form m-SBF. Collagen-mica substrates were prepared with adsorbed proteins as described above. However, the discs were incubated with only one exposure concentration for each SIBLING protein to eliminate the need for normalization between different protein-collagen substrates due to differences in the amount of adsorbed protein. Specifically, 10 μg/mL BSP, 50 μg/mL OPN, and 32.5 μg/mL DPP were used. Heat denatured BSA (1 mg/mL) samples were also prepared as a control. Following the protein adsorption step, the discs were then washed with 18.2 MΩ-cm water to remove non-specifically adsorbed proteins and placed into the m-SBF for 5, 10, or 24 hours at 37 °C. Following incubation, the samples were removed and rinsed with ultrapure water and dried with filtered air before mineral characterization.

Mineral morphology analysis

The morphology of the minerals formed in SBF was examined using AFM. AFM was performed on an Agilent 5400 with silicon cantilevers having a force constant of 0.2 N/m and a resonant frequency of 13 kHz. Images were obtained in contact mode with a resolution of 1024×1024 pixels at a rate of 3.0 lines/second using a 10 μm scanner. Images were simultaneously recorded in topography and deflection modes. All images were acquired in air at room temperature. Gwyddion freeware was used to view and analyze the images.[25] Roughness parameters for each image were calculated in Gwyddion after plane flattening. Three images were captured and analyzed for three independently prepared samples at each protein and mineralization time point combination (n=9).

Mineral composition analysis

Substrate surfaces were demineralized using a modified version of a previously established procedure.[28] Briefly, mineralized mica-collagen-protein substrates were demineralized by soaking the sample in 1.0 M nitric acid for 30 minutes. The acid solution was then neutralized with an equal amount of 1.0 M sodium hydroxide. The resulting solution from each disc was used in the calcium and phosphate photochemical assays. Commercial colorimetric assay kits were used to determine the ionic calcium and phosphate concentrations in the demineralization solutions. The QuantiChrom calcium assay was used for calcium tests while the PiPer assay was used for determining phosphate concentrations. Standard calibration curves were constructed for both assay kits using solutions with known concentrations following the manufacturer's recommended protocols. The QuantiChrom

assay forms a blue colored complex with calcium via a phenolsulphonephthalein dye. The PiPer assay kit forms resorufin in an amount proportional to the amount of phosphate present in solution by enzymatic digestion of sugars, after which the resorufin concentration can be measured spectrophotometically. Samples were analyzed with a PowerWave XS2 multi-well plate reader from BioTek (Winooski, VT) at 612 nm and 565 nm for the calcium and phosphate assays, respectively. Data collection was performed using Gen5 1.07 (BioTek). Ca:P ratios were calculated after determining Ca^{2+} and PO_4^{3-} concentrations for individual samples. A minimum of 2 samples were analyzed from each of three independent experiments ($n \geq 7$).

Data Analysis

All of the data are presented as the average ± standard error of the mean of all of the samples for a given data set. The results were identified as being statistically significant from each other at a 95% confidence interval ($p < 0.05$) using a one-way analysis of variance (ANOVA) test. The statistical analysis was conducted using OriginPro 8.5 software.

Results and Discussion

Collagen Substrate Characterization

In order to accurately assess the mineralization induction properties of OPN, BSP, and DPP it is important to conduct the study on a substrate that mimics the native structure of developing bone. Previously it was shown that tropocollagen molecules self-assemble into loosely aligned collagen fibrils on freshly cleaved mica under carefully controlled conditions.[20] This was confirmed in this study by exposing freshly cleaved mica disks to a 0.3 mg/mL solution of collagen in KCl-Tris buffer. Figure 1a shows a representative AFM image which clearly demonstrates that a loosely aligned coating of collagen fibrils was obtained with this self-assembly technique. The fibrils exhibited a width of ~100 nm and under higher magnification the prototypical 67 nm *D*-periodicity banding of collagen fibrils was observed (data not shown). Figure 1b shows a lower magnification AFM image, to demonstrate the uniformity of this coating across the surface. Figure 1c shows a representative AFM image of the bare mica control surface to clearly demonstrate that the topographical features seen in Figures 1 a-b result from the collagen coating. These results indicate that this two dimensional collagen fibril platform is a good *in vitro* analog to developing bone, making it suitable for probing the biomineralization induction properties of the SIBLING proteins. Because the collagen formation procedures were based on previously established methods, no further characterization of the collagen substrate was performed.

Protein Adsorption Isotherms

In order to compare the effects of the different SIBLING proteins on mineralization, it is important to identify conditions that lead to identical amounts of the proteins being present on the substrate to eliminate the need for normalization. This was accomplished by developing ^{125}I radiolabeled adsorption isotherms for BSP, OPN, and DPP on the collagen-mica substrates. The adsorbed amount of protein was calculated by using the specific measured radioactivity of each protein solution before adsorption and the activity of the collagen-mica substrate after protein adsorption and extensive rinsing. The resulting adsorption isotherms are shown in Figure 2. In this Figure it can be observed that BSP has the highest affinity for the collagen-mica substrate at lower exposure concentrations. DPP and OPN had similar binding profiles with DPP having slightly higher adsorption levels at each concentration. However, at the highest exposure concentration of 100 μg/mL, all three proteins converged to a similar amount of specifically adsorbed proteins. These isotherms were then used to determine exposure concentrations that resulted in identical amounts of

adsorbed protein for each of the three proteins at an intermediate or lower exposure concentration. A low to intermediate concentration was chosen to better mimic the native concentration of these proteins in bone tissue.[3-5,17] The dotted lines in Figure 2 highlight the concentrations that were identified and used in the subsequent mineralization study for each of the three proteins. Specifically, concentrations of 10 μg/mL BSP, 32.5 μg/mL DPP, and 50 μg/mL OPN were used to obtain ~1.3 ng of adsorbed protein per mm^2 of collagen-mica substrate.

Following protein adsorption, additional control AFM images were collected to identify topological features that result from protein adsorption. Figure 1d shows a representative image for the collagen coated substrates following BSA adsorption. This Figure is representative of all of the substrates following protein adsorption from the three SIBLING proteins as well (data not shown). It can be seen that there are no obvious topological changes as a result of the protein adsorption process. Therefore, it can be concluded that any new topological features seen by AFM following exposure to m-SBF are a mineralization product.

Mineral morphology analysis

Following the identification of exposure conditions that resulted in equal amounts of adsorbed BSP, OPN, and DPP, mineralization induction studies were initiated. These studies were conducted by exposing the substrates to Oyane *et al.*'s m-SBF, which closely mimics the native ion concentrations in plasma without the biological components.[27] The subsequent mineralization was characterized following 5, 10, and 24 hours of immersion in the m-SBF. Figures 3, 4, and 5 show representative AFM images for each of the proteins following 5, 10, and 24 hours of mineralization, respectively. Additionally, the average roughness measurements determined from multiple AFM images for each of the protein-time point combinations are summarized in Figure 6.

In order to monitor for bulk mineralization effects, control surfaces were completed with heat denatured BSA as a non-mineralizing protein. As seen in Figure 3a, after 5 hours of immersion in m-SBF, the BSA coated surfaces showed some bulk mineralization effects. This is evident when comparing the morphology of the collagen substrate before (Figure 1a and 1d) and after mineralization. It is more challenging to distinguish the individual fibers following exposure to m-SBF. However, there are no observable changes from the 5 hour time point to the 10 and 24 hour time points as seen in Figures 4a and 5a. Interestingly, while there are no obvious qualitative differences in the mineralization across the BSA samples there is a difference in the surface roughness across the different time points, including a statistically significant drop off in the roughness following 24 hours of exposure to m-SBF, as compared to 10 hours of exposure. This is shown in Figure 6. The likely explanation for these results is that bulk precipitation occurs during the entirety of the m-SBF exposure. Initially bulk precipitation increases the surface roughness, through the 10 hour time point. Beyond that, bulk precipitates may be more likely to settle into features on the sample surface, ultimately leading to a reduction in the surface roughness.

When examining the mineralization on the samples with BSP there were no real qualitative differences that could be observed as compared to the BSA control samples at any of the time points. In Figures 3b, 4b, and 5b it can be seen that there appears to be a minimal degree of mineralization, likely due to precipitation from solution. However, when comparing the quantifiable surface roughness, a different trend from that seen for the BSA controls was seen. In Figure 6, it can be seen that there is a drop off in the surface roughness at the 10 hour time point as compared to the 5 and 24 hour time points. However, this difference was not statistically significant and may simply represent sample variability.

The mineralization results seen in the presence of DPP were in stark contrast to the results seen for both BSA and BSP. As seen in Figures 3c, 4c, and 5c distinct mineral nodules were seen at all time points on the DPP samples. Furthermore, these mineral nodules appear to correlate well with the collagen fibrils. They also seem to increase slightly in size as the m-SBF exposure time is increased and there does not appear to be a change in the relative number of mineral nodules present as a function of time. The roughness measurements conducted across multiple samples also indicate that there are no significant differences between the samples at any of the time points. This can be seen in Figure 6. These results suggest that there is a uniform mineralization process occurring on these samples. Additionally, the roughness value is similar to the maximum values seen with all of the other protein samples. It is believed that the formation of specific mineral nodules depleted the ion concentration in the bulk solution, effectively preventing the bulk precipitation believed to occur in the presence of both BSA and BSP.

The final SIBLING protein that was tested was OPN and representative mineral morphologies can be seen in Figures 3d, 4d, and 5d. The substrates treated with OPN appeared to have some mineral formation after 5 hours. It also appears that the mineral is formed either on top of or alongside the collagen fibrils. As the mineralization time was increased, these minerals appeared to become less distinct. These observations correlate with the roughness measurements shown in Figure 6. The roughness was seen to steadily decrease over time. Interestingly, there is no difference in the surface roughness between the original collagen substrate and the OPN substrate following 24 hours of exposure to m-SBF. Additionally, this roughness value was statistically significantly lower than that found following 5 hours of exposure to m-SBF. These results may suggest that OPN plays a role in the initial surface mineralization, but that the minerals that are formed mature over time. This would be consistent with the current perception of OPN's role in biomineralization.

Mineral composition analysis

After characterizing the morphology, surface coverage, and roughness of the minerals, photochemical assays were used to quantify the amount of calcium and phosphate ions present under all of the conditions examined above. The complete demineralization of the samples by the nitric acid procedures was also confirmed by AFM (data not shown). The absolute concentrations for calcium and phosphate as determined with this approach can be seen in Figures 7a and 7b, respectively.

The BSA coated surfaces exhibited a high concentration of calcium relative to the three SIBLING proteins at 5 and 24 hours as shown in Figure 7a. BSA has been shown to chelate Ca^{2+}, so this result was not unexpected.[29] Interestingly, the relative calcium concentration following 10 hours of m-SBF exposure showed a significantly lower amount of Ca^{2+} ions relative to the other time points. This is even more surprising when combined with the fact that the 10 hour samples had the highest surface roughness of the BSA samples. There were no differences between the other two time points, although there was slightly more average calcium present after 5 hours. The phosphate concentration results showed a similar trend with the greatest measured concentrations occurring on samples following 5 hours of m-SBF exposure and the lowest concentrations following 10 hours of exposure.

The measured calcium concentrations from samples with BSP following 5 hours of exposure to m-SBF were noticeably lower than those seen with BSA. A significant increase in the amount of calcium was seen at the 10 hour time point, with a nearly identical amount of calcium present following 24 hours. Both of these points were statistically greater than the concentration at the 5 hour time point. These maximum calcium concentrations were similar to those seen in the presence of BSA following 24 hours of exposure to m-SBF and they were the highest measured calcium concentrations found for minerals formed in the

presence of any of the SIBLING proteins examined in this study. As seen in Figure 7b, the phosphate concentrations from minerals formed in the presence of BSP were relatively constant across all of the time points examined. There was a slightly lower level at the 10 hour time point, but this result was not significantly different. There were also no relative differences between the BSP and BSA samples in terms of the phosphate concentrations.

The calcium and phosphate concentrations found from minerals formed in the presence of DPP exhibited trends that match what would be expected of a mineralizing system. If active mineralization was occurring it would be expected that the absolute concentration of Ca^{2+} and PO_4^{3-} would continually increase over time. The concentrations of both ions showed continually increasing levels with increased exposure time only in the presence of DPP. However, it is interesting to note that the absolute values of the calcium concentrations are noticeably lower than the maximum measurements for both BSA and BSP. At the same time, the phosphate measurements at the 10 and 24 hour time points were the highest of any of the SIBLING proteins. These results are also consistent with the obvious mineral nodule formation seen on the AFM images. Furthermore, the continual increase in the ion concentrations suggests that the minerals are either continually growing or they are maturing with increased m-SBF exposure time.

The relative concentration of calcium in minerals formed in the presence of OPN also showed a continual increase over time to similar levels as those seen in the presence of DPP. However, the phosphate concentration levels peaked in the minerals formed after 10 hours of m-SBF exposure. The amount of phosphate was slightly higher after 24 hours as compared to 5 hours of exposure. It is interesting to consider these results in combination with the roughness results seen in Figure 6. The fact that the calcium levels continued to increase with exposure time while the roughness continued to decrease is consistent with the perception that OPN plays a role in mineral maturation.

The final characterization that was conducted was the determination of the calcium to phosphate ratio for individual samples. Calcium phosphate minerals are often identified based on their calcium to phosphate ratio and the mineral component of bone has been seen to have a ratio of approximately 1.49:1.[30] In this study, the Ca:P ratio was determined for the individually demineralized samples using a normalization factor for the calcium concentration. This was necessary because mica is known to contain calcium ions that could be removed during the demineralization process. In order to determine the normalization factor, collagen-mica substrates were prepared, but not exposed to SBF. Then these samples were subjected to the demineralization, calcium assay, and phosphate assay processes. Upon completion, it was found that the collagen-mica substrate produced 7.93 ± 5.08 μmol of calcium (n=5), while there were no detectable levels of phosphate present. This value for calcium was then used to reduce the absolute calcium concentration values before the Ca:P ratio was determined.

The Ca:P ratios of the minerals formed with each of the proteins at each of the time points examined are shown in Figure 8. The control BSA sample had a Ca:P ratio trend that was similar to that seen for the Ca concentration. Following 5 and 24 hours of m-SBF exposure there were similar Ca:P ratios found, but there was a noticeable decrease in the ratio measured following 10 hours of exposure. Conversely, in the presence of all three of the SIBLING proteins, the Ca:P ratio exhibited a peak following 10 hours of m-SBF exposure with the minimum ratio being found following 5 hours of exposure. There were no statistically significant differences in the maximum values found for any of the proteins tested. Interestingly, under all of the conditions examined in this investigation, the Ca:P ratios were much higher than those found in native bone minerals. This could be due to ion-protein interactions, as all of the SIBLING proteins have been shown to have strong calcium

binding properties.[1-3,12,31] It is also possible that the high Ca:P ratio could be an indication that immature bone minerals are being formed. On-going research efforts are focused on determining the crystal state of the minerals to better understand the SIBLING protein induced biomineralization process seen under the conditions examined here.

Conclusions

In this investigation the biomineralization induction properties of three SIBLING proteins (OPN, BSP, and DPP) were investigated on a biomimetic collagen type I fibril substrate. The mineralization experiments were conducted under conditions where identical amounts of adsorbed protein were specifically bound to a loosely aligned collagen fibril coating. The mineral morphology was characterized using AFM and the composition was characterized using photochemical assays. While minerals were observed in the presence of each of the SIBLING proteins and the control substrate with adsorbed BSA, only the samples with adsorbed DPP had distinct mineral nodules that mimic those seen in developing bone. Furthermore, all of the minerals found under the conditions used in this investigation had Ca:P ratios that were significantly larger than what has been found in native bone tissue. When taken together, these results suggest that the SIBLING proteins can mediate the biomineralization process. However, it is likely that the minerals mature over a longer period of time that what was examined in this study or following exposure to a second SIBLING protein.

Acknowledgments

We would like to acknowledge Dr. Patrick Pinhero and his group for the use of his AFM and Dr. Duane Keisler for his assistance with the radiolabeling studies. This study was supported by a University of Missouri System Research Board Grant #CB000422 and by the MU College of Engineering (MTB) and by NIH Grant DE005092 (CQ).

References

1. Gokhale, JA.; Boskey, AL.; Robey, PG. The Biochemistry of Bone. In: Marcus, R.; F, D.; Kelsey, J., editors. Osteoporosis. Second. San Diego: Academic Press; 2001. p. 107-188.
2. George A, Veis A. Phosphorylated Proteins and Control over Apatite Nucleation, Crystal Growth, and Inhibition. Chemical Reviews. 2008; 108(11):4670–4693. [PubMed: 18831570]
3. Ganss B, Kim RH, Sodek J. Bone sialoprotein. Critical Reviews in Oral Biology and Medicine. 1999; 10(1):79–98. [PubMed: 10759428]
4. Sodek J, Ganss B, McKee MD. Osteopontin. Critical Reviews in Oral Biology and Medicine. 2000; 11(3):279–303. [PubMed: 11021631]
5. Yamakoshi Y. Dentin sialophosphoprotein (DSPP) and dentin. Journal of Oral Biosciences. 2008; 50(1):33–44. [PubMed: 20037676]
6. Prasad M, Butler WT, Qin C. Dentin sialophosphoprotein in biomineralization. Connective Tissue Research. 2010; 51(5):404–417. [PubMed: 20367116]
7. Butler W. Macromolecules of extracellular matrix: Determination of selective structures and their functional significance. Connective Tissue Research. 2008; 49(6):383–390. [PubMed: 19085238]
8. Goldberg HA, Warner KJ, Li MC, Hunter GK. Binding of bone sialoprotein, osteopontin and synthetic polypeptides to hydroxyapatite. Connective Tissue Research. 2001; 42(1):25–37. [PubMed: 11696986]
9. Puleo DA, Nanci A. Understanding and controlling the bone-implant interface. Biomaterials. 1999; 20(23-24):2311–2321. [PubMed: 10614937]
10. Roach HI. Why does bone matrix contain non-collagenous proteins? The possible roles of osteocalcin, osteonectin, osteopontin and bone sialoprotein in bone mineralisation and resorption. Cell Biology International. 1994; 18(6):617–628. [PubMed: 8075622]

11. Veis A. Mineral-matrix interactions in bone and dentin. Journal of Bone and Mineral Research. 1993; 8(SUPPL. 2):S493–S497. [PubMed: 8122518]
12. Giachelli CM, Steitz S. Osteopontin: a versatile regulator of inflammation and biomineralization. Matrix Biology. 2000; 19(7):615–622. [PubMed: 11102750]
13. Wilson CJ, Clegg RE, Leavesley DI, Pearcy MJ. Mediation of biomaterial-cell interactions by adsorbed proteins: A review. Tissue Engineering. 2005; 11(1-2):1–18. [PubMed: 15738657]
14. Baht GS, Hunter GK, Goldberg HA. Bone sialoprotein-collagen interaction promotes hydroxyapatite nucleation. Matrix Biology. 2008; 27(7):600–608. [PubMed: 18620053]
15. Gordon JAR, Tye CE, Sampaio AV, Underhill TM, Hunter GK, Goldberg HA. Bone sialoprotein expression enhances osteoblast differentiation and matrix mineralization in vitro. Bone. 2007; 41(3):462–473. [PubMed: 17572166]
16. Qin C, Brunn JC, Cadena E, Ridall A, Tsujigiwa H, Nagatsuka H, Nagai N, Butler WT. The expression of dentin sialophosphoprotein gene in bone. Journal of Dental Research. 2002; 81(6): 392–394. [PubMed: 12097430]
17. MacDougall M, Simmons D, Luan X, Nydegger J, Feng J, Gu TT. Dentin Phosphoprotein and Dentin Sialoprotein Are Cleavage Products Expressed from a Single Transcript Coded by a Gene on Human Chromosome 4. Journal of Biological Chemistry. 1997; 272(2):835–842. [PubMed: 8995371]
18. Milan AM, Sugars RV, Embery G, Waddington RJ. Adsorption and interactions of dentine phosphoprotein with hydroxyapatite and collagen. European Journal of Oral Sciences. 2006; 114(3):223–231. [PubMed: 16776772]
19. Bernards MT, Qin C, Ratner BD, Jiang S. Adhesion of MC3T3-E1 cells to bone sialoprotein and bone osteopontin specifically bound to collagen I. Journal of Biomedical Materials Research Part A. 2008; 86A(3):779–787. [PubMed: 18041732]
20. Jiang F, Hörber H, Howard J, Müller DJ. Assembly of collagen into microribbons: effects of pH and electrolytes. Journal of Structural Biology. 2004; 148(3):268–278. [PubMed: 15522775]
21. Prince CW, Oosawa T, Butler WT, Tomana M, Bhown AS, Bhown M, Schrohenloher RE. Isolation, characterization, and biosynthesis of a phosphorylated glycoprotein from rat bone. Journal of Biological Chemistry. 1987; 262(6):2900–2907. [PubMed: 3469201]
22. Qin C, Brunn JC, Jones J, George A, Ramachandran A, Gorski JP, Butler WT. A comparative study of sialic acid-rich proteins in rat bone and dentin. European Journal of Oral Sciences. 2001; 109(2):133–141. [PubMed: 11347657]
23. Qin C, Brunn JC, Baba O, Wygant JN, McIntyre BW, Butler WT. Dentin sialoprotein isoforms: Detection and characterization of a high molecular weight dentin sialoprotein. European Journal of Oral Sciences. 2003; 111(3):235–242. [PubMed: 12786955]
24. Huang B, Sun Y, MacIejewska I, Qin D, Peng T, McIntyre B, Wygant J, Butler WT, Qin C. Distribution of SIBLING proteins in the organic and inorganic phases of rat dentin and bone. European Journal of Oral Sciences. 2008; 116(2):104–112. [PubMed: 18353003]
25. Liu L, Chen S, Giachelli CM, Ratner BD, Jiang S. Controlling osteopontin orientation on surfaces to modulate endothelial cell adhesion. Journal of Biomedical Materials Research - Part A. 2005; 74(1):23–31. [PubMed: 15920735]
26. Feng C, Keisler DH, Fritsche KL. Dietary omega-3 polyunsaturated fatty acids reduce IFN-γ receptor expression in mice. Journal of Interferon and Cytokine Research. 1999; 19(1):41–48. [PubMed: 10048767]
27. Oyane A, Onuma K, Ito A, Kim HM, Kokubo T, Nakamura T. Formation and growth of clusters in conventional and new kinds of simulated body fluids. Journal of Biomedical Materials Research. 2003; 64A(2):339–348. [PubMed: 12522821]
28. Gungormus M, Fong H, Kim IW, Evans JS, Tamerler C, Sarikaya M. Regulation of in vitro Calcium Phosphate Mineralization by Combinatorially Selected Hydroxyapatite-Binding Peptides. Biomacromolecules. 2008; 9(3):966–973. [PubMed: 18271563]
29. Dorozhkin SV, Dorozhkina EI. The influence of bovine serum albumin on the crystallization of calcium phosphates from a revised simulated body fluid. Colloids and Surfaces A: Physicochemical and Engineering Aspects. 2003; 215(1-3):191–199.

30. Lu HB, Campbell CT, Graham DJ, Ratner BD. Surface characterization of hydroxyapatite and related calcium phosphates by XPS and TOF-SIMS. Analytical Chemistry. 2000; 72(13):2886–2894. [PubMed: 10905323]

31. Omelon SJ, Grynpas MD. Relationships between Polyphosphate Chemistry, Biochemistry and Apatite Biomineralization. Chemical Reviews. 2008; 108(11):4694–4715. [PubMed: 18975924]

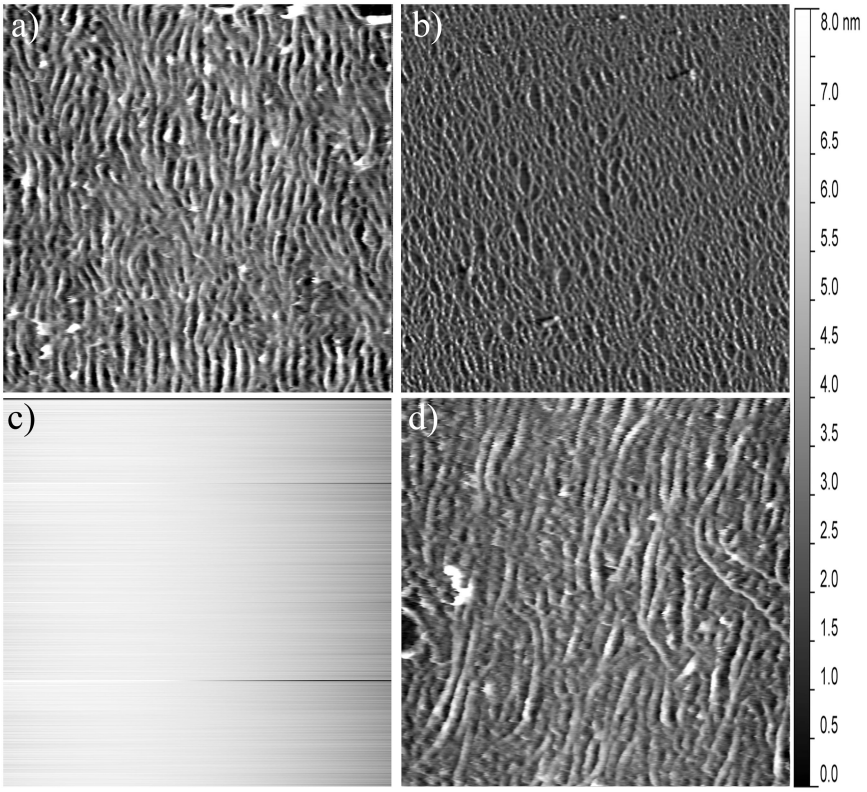

Figure 1.

Representative AFM images showing a) a 2.5 μm × 2.5 μm section of the collagen-mica substrate and b) a 10 μm × 10 μm section of the collagen-mica substrate, both following the self-assembly of a coating of loosely aligned collagen fibrils; c) a 2.5 μm × 2.5 μm section of the bare mica substrate before collagen fibril assembly; and d) 2.5 μm × 2.5 μm section of the collage-mica substrate following exposure to 1 mg/mL of heat denatured BSA.

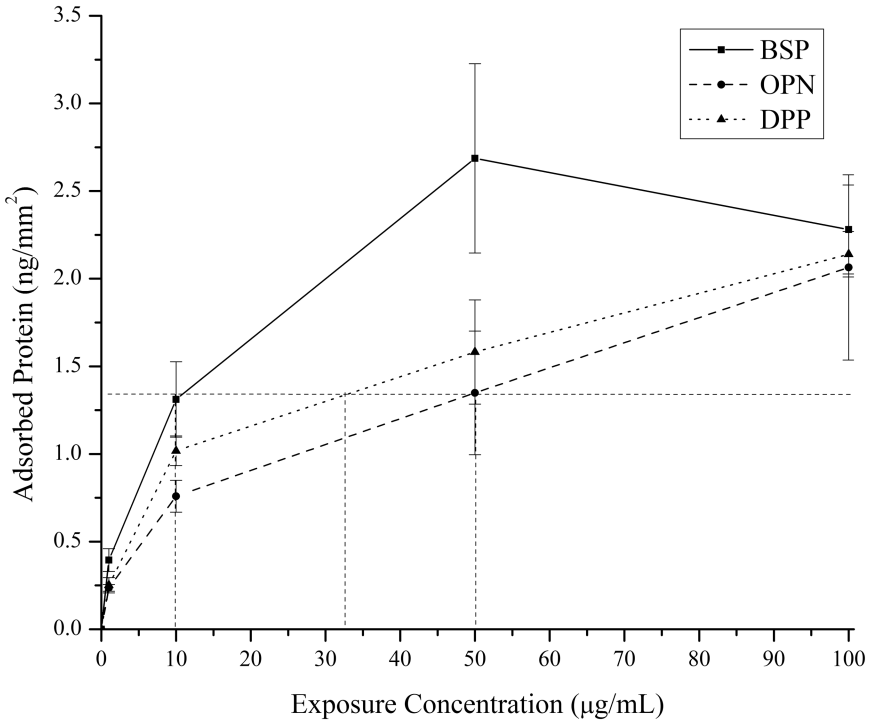

Figure 2.

^{125}I radiolabeled adsorption isotherms for BSP (squares), OPN (circles), and DPP (triangles) on the collagen-mica substrate. The dotted lines indicate the exposure concentrations used for each of the three proteins in the subsequent mineralization studies. The data is presented as the mean ± standard error of the mean from three independently prepared samples (n=3).

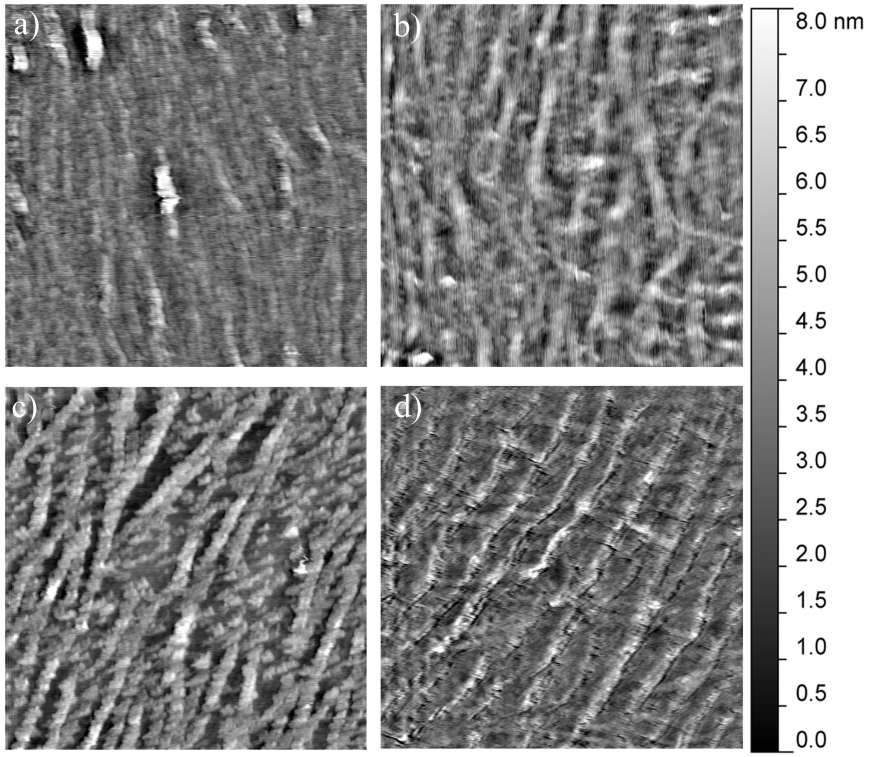

Figure 3.

Representative 2.5 μm × 2.5 μm AFM images of the mineralization induced on the collagen-mica substrate after 5 hours of immersion in SBF in the presence of (a) 1 mg/mL heat denatured BSA, (b) 10 μg/mL BSP, (c) 35.5 μg/mL DPP, and (d) 50 μg/mL OPN.

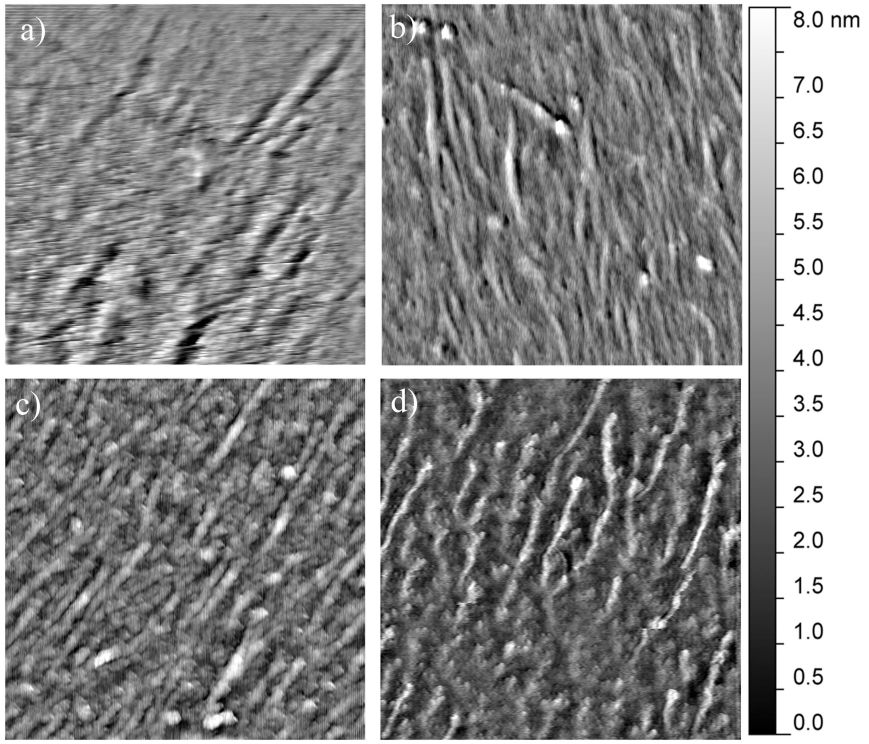

Figure 4.

Representative 2.5 μm × 2.5 μm AFM images of the mineralization induced on the collagen-mica substrate after 10 hours of immersion in SBF in the presence of (a) 1 mg/mL heat denatured BSA, (b) 10 μg/mL BSP, (c) 35.5 μg/mL DPP, and (d) 50 μg/mL OPN.

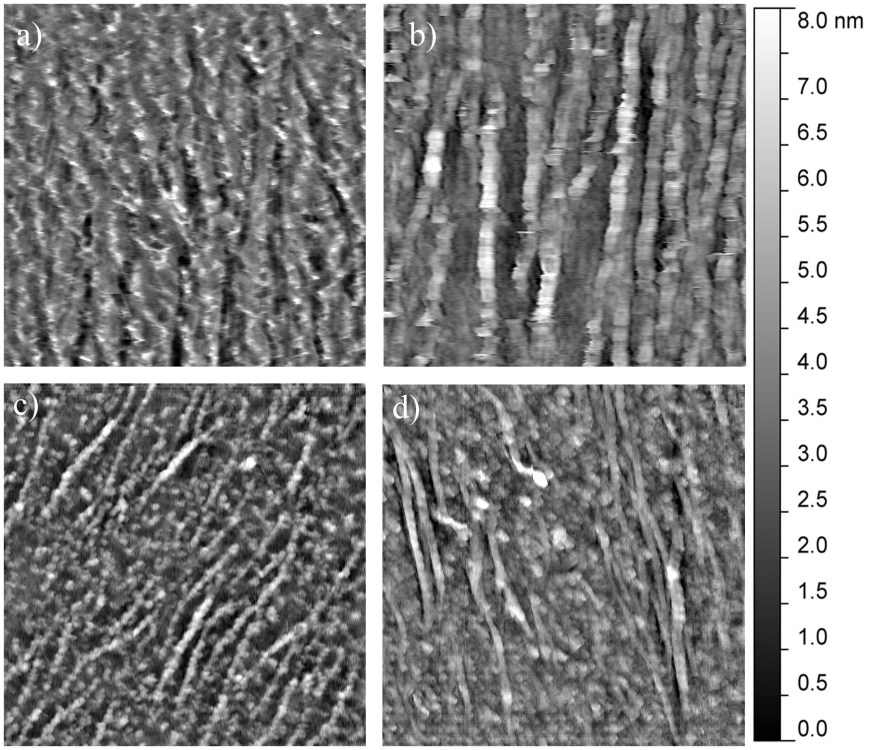

Figure 5.

Representative 2.5 μm × 2.5 μm AFM images of the mineralization induced on the collagen-mica substrate after 24 hours of immersion in SBF in the presence of (a) 1 mg/mL heat denatured BSA, (b) 10 μg/mL BSP, (c) 35.5 μg/mL DPP, and (d) 50 μg/mL OPN.

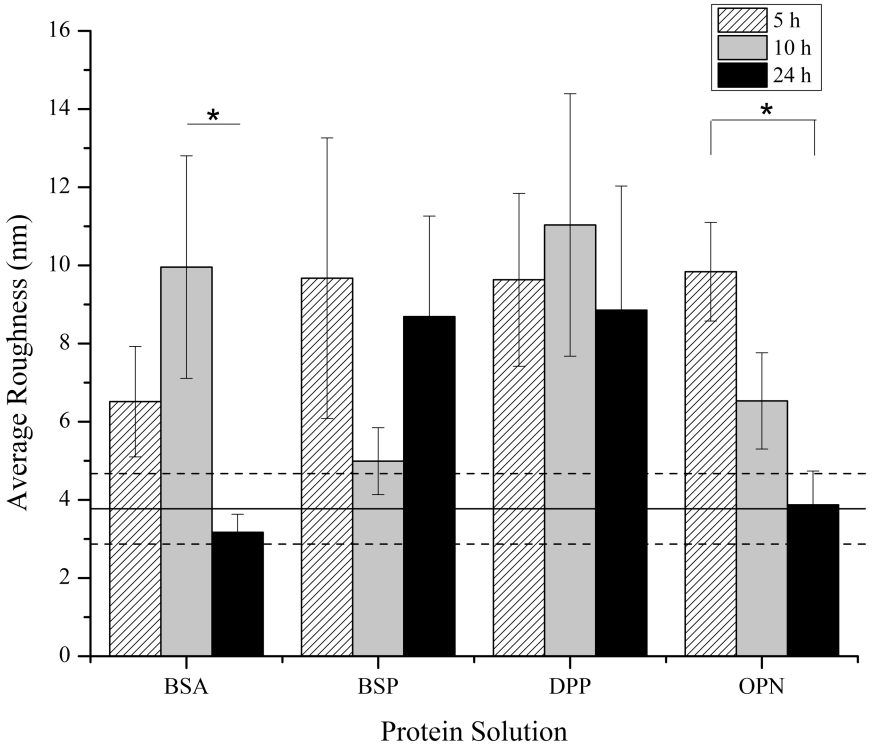

Figure 6.

Mean ± standard error of the mean of the surface roughness of the mineralized substrates after immersion in SBF for 5, 10, and 24 hours in the presence of proteins (n=9). The solid horizontal line represents the average roughness of the original collagen substrate prior to protein adsorption and mineralization and the dashed lines represent the standard error of the mean for this control. A * represents a statistically significant difference between the surfaces being compared at a 95% confidence interval ($p<0.05$).

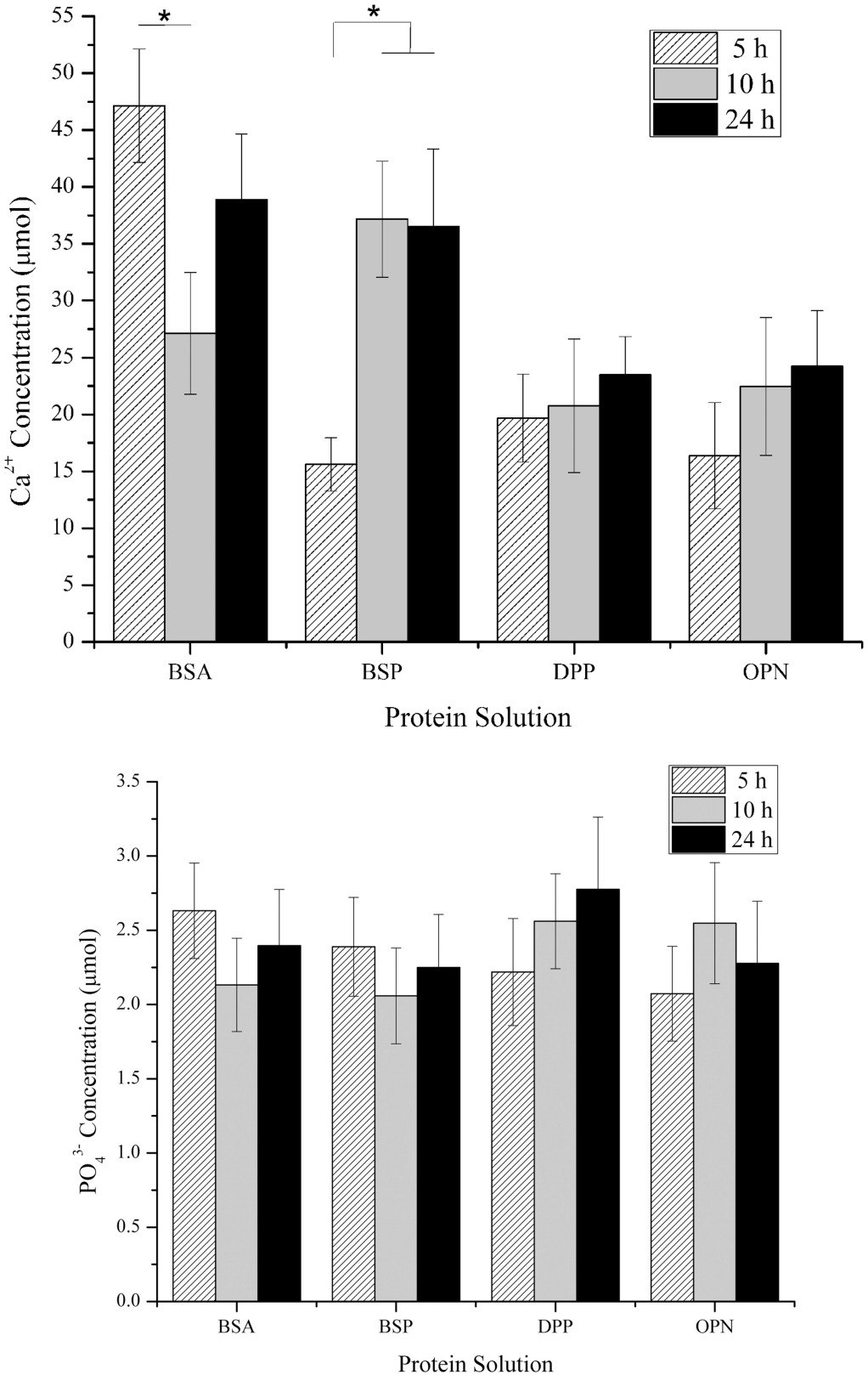

Figure 7.

Mean ± standard error of the mean of the measured (a) Ca^{2+} and (b) PO_4^{3-} concentrations following the demineralization of the collagen-mica substrates after immersion in SBF for 5, 10, and 24 hours in the presence of adsorbed BSA, BSP, DPP, or OPN. The concentrations were determined using calcium and phosphate assay kits for a minimum of 7 independently prepared samples ($n \geq 7$). A * represents a statistically significant difference between the surfaces being compared at a 95% confidence interval ($p < 0.05$).

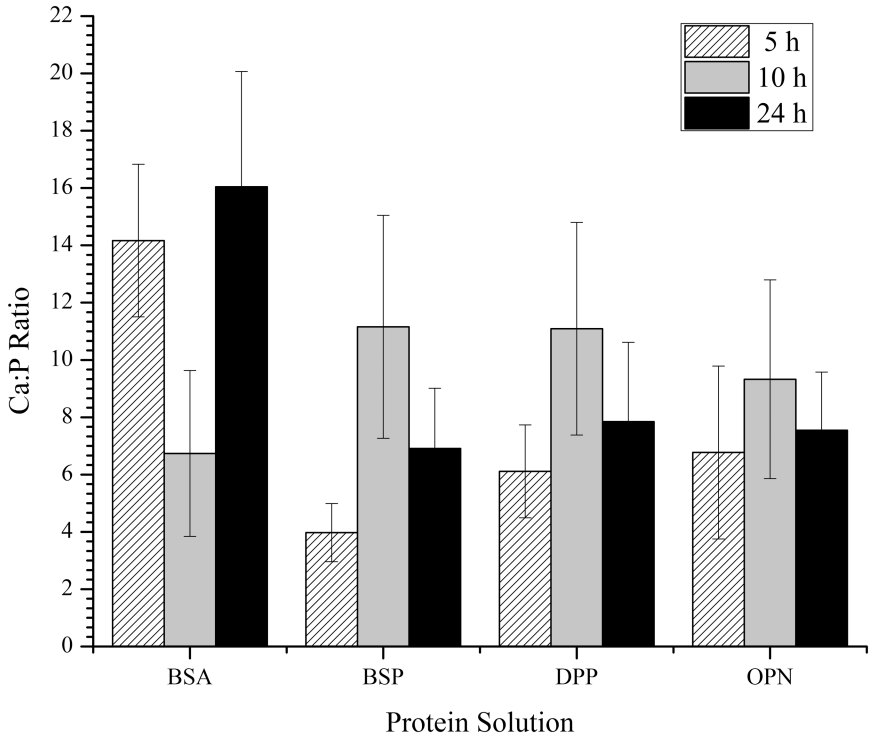

Figure 8.

Mean ± standard error of the mean of the normalized Ca:P ratio following the demineralization of the collagen-mica substrates after immersion in SBF for 5, 10, and 24 hours in the presence of adsorbed BSA, BSP, DPP, or OPN. The ratio for a minimum of 5 independently prepared samples were determined under each condition (n>5).

Table 1

Preparation conditions for 500 mL of SBF using Oyane *et al.*'s recipe for m-SBF.[27]

Reagent	Quantity (g)
NaCl	2.7015
$NaHCO_3$	0.252
Na_2CO_3	0.213
KCl	0.1125
K_2HPO_4	0.115
$MgCl_2{\cdot}6H_2O$	0.1555
HEPES[a]	8.946[b]
$CaCl_2$	0.1465
Na_2SO_4	0.036
1.0 M NaOH	*c*

[a] 2-(4-(2-hydroxyethyl)-1-piperazinyl)ethanesulfonic acid.

[b] HEPES was dissolved in 50 mL of 0.2 M NaOH before addition

[c] Added until pH 7.4.